Journal of Materials Chemistry A

RSC Publishing

PAPER

View Article Online
View Journal | View Issue

Cite this: J. Mater. Chem. A, 2013, 1, 10875

A new fabrication method of an intermediate temperature proton exchange membrane by the electrospinning of CsH_2PO_4

Asier Goñi-Urtiaga,*[a] Keith Scott,[a] Sara Cavaliere,[b] Deborah J. Jones*[b] and Jacques Roziére[b]

Received 10th May 2013
Accepted 12th July 2013

DOI: 10.1039/c3ta11851g

www.rsc.org/MaterialsA

A novel method for the fabrication of an intermediate temperature proton conducting composite membrane was developed. Cesium dihydrogen phosphate, CsH_2PO_4 (CDP), was electrospun to obtain a highly interconnected proton conducting fibre mat. CsH_2PO_4 was heat treated above its dehydration temperature ($T_{dehy} \sim 230$ °C) in order to induce a partial polymerisation. The partially polymerised material produced a viscous aqueous solution which could be electrospun in the absence of a carrier polymer, thus leading to pure inorganic fibres. The electrospun fibre mats were characterised in terms of composition, structure and morphology by XRD, MAS NMR and SEM and their proton conductivity determined by electrochemical impedance spectroscopy. The electrospun fibres (CDP_f) showed a maximum proton conductivity of 8×10^{-3} S cm^{-1} at 250 °C.

1 Introduction

Great effort has been made in materials science to develop new materials to allow an increase in the operating temperature of proton exchange membrane fuel cells (PEMFCs) and water electrolysers (PEMWEs). An increase in the operating temperature improves the thermodynamic efficiency and enhances the kinetics of the electrochemical reactions and the catalyst tolerance to CO poisoning. Water management in these devices is also greatly simplified when operating above 100 °C.

Solid acids have attracted great interest in the last decade due to their high proton conductivity (10^{-2} to 10^{-3} S cm^{-1}) at the intermediate temperature range (150–300 °C).[1–8] Among them CsH_2PO_4 (CDP) has been proven to be a most promising material in terms of proton conductivity (2×10^{-2} S cm^{-1} at $T > 230$ °C) and chemical stability.[9,10] The properties of CDP make it desirable to use as a solid electrolyte in intermediate temperature electrochemical devices.[1,11] However, the inorganic nature of CDP makes it difficult to build a thin and robust membrane with low ohmic resistance. Several attempts have been made to fabricate a thin pellet[10] or composite materials based on CDP.[12–16] In the present work a new fabrication method of a composite membrane based on the electrospinning of CDP is proposed.

Electrospinning is a technique used to produce polymeric or hybrid fibres in the micrometre to nanometre scale.[17,18] The principle of this technique is to apply a high potential to a drop of a polymer solution such that the repulsive electrical forces overcome the surface tension of the drop. A charged jet of the solution is then ejected onto a grounded collector covered by an aluminium foil allowing the evaporation of the solvent and the formation of solid thin fibres, Fig. 1.

A CDP solution in water cannot be electrospun because of the low viscosity and charging of the solution when a high voltage is applied. The addition of a carrier polymer to the solution could provide a way to electrospin CDP fibres but this would imply further treatment of the produced fibres to eliminate the polymer, either thermally or by washing. This step would affect the integrity of the fibres in terms of morphology and composition. For this reason a different method to electrospin CDP, based on the condensation of phosphates, was developed.

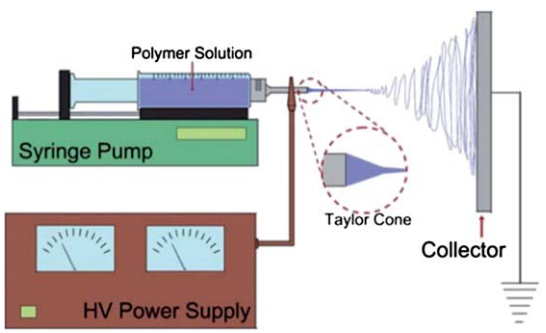

Fig. 1 Scheme of a conventional electrospinning set-up.[17]

[a]Newcastle University, Chemical Engineering & Advanced Materials, Mertz Court, NE1 7RU, Newcastle upon Tyne, UK. E-mail: asier.goni@newcastle.ac.uk; Tel: +44 (0) 191 222 3070

[b]ICGM, UMR 5253, Equipe AIME Université Montpellier II, 2 Place Eugène Bataillon, CC 1502 34095 Montpellier CEDEX 5, France. E-mail: deborah.jones@univ-montp2.fr; Fax: +33(0)467143304; Tel: +33(0)467143330

CDP, similar to the majority of the phosphate-based solid acids,[1,10] undergoes a dehydration/polymerisation reaction (Reaction (1)) at a temperature higher than its so-called super-protonic phase transition temperature. By this reaction the material loses its constituent water, generating successively longer chains of condensed phosphates[19] leading to the formation of pyro- and poly-phosphates ($CsH_xP_yO_z$) until its complete dehydration to cesium metaphosphate ($CsPO_3$).

$$CsH_2PO_4(s) \rightarrow CsH_{2-2x}PO_{4-x}\,(s) + xH_2O\,(g),\ (0 < x \leq 1) \quad (1)$$

When this polymerised material is dissolved in water it gives a transparent viscous solution. The viscosity of this solution allows it to be electrospun in the absence of any carrier polymer or additive making it possible to generate pure inorganic fibres of this salt in one step.

This method is proposed here for the elaboration of a dense highly interconnected CDP fibre-mat. The later consolidation of the mat by addition of a thermostable polymer to further improve the mechanical properties and occlude porosity then leads to a new fabrication method of a medium temperature proton conducting membrane.

2 Experimental

2.1 Sample preparation

CsH_2PO_4 (CDP) synthesis was carried out by reacting Cs_2CO_3 (Aldrich, 99.0%) and H_3PO_4 (Sigma-Aldrich, ACS >85 wt% aq. solution) in a molar ratio of 1 : 2. The reaction was performed in aqueous solution at room temperature. Polycrystalline powder of CDP was obtained by slow addition of the aqueous solution into methanol. The samples were dried in an oven at 90 °C for 12 h and ground in a mortar. The polycrystalline powder of CDP was then heat-treated to induce the dehydration reaction (Reaction (1)). The thermal treatment was carried out in a furnace at 300 °C for 3 h using a heating ramp of 10 °C min^{-1}. These treatment conditions were chosen as they induced the lowest degree of dehydration/polymerisation needed to electrospin CDP into fibres.

The resulting partially polymerised CsH_2PO_4 powder (CDP_p) was then dissolved in DI water to a concentration of 2.25 g ml^{-1}. This concentration provided suitable viscosity for continuous fibre formation by electrospinning. The solution of CDP_p was then electrospun by the electrospinning device onto a grounded collector covered by an aluminium foil. The output solution rate of the needle was 0.3 ml h^{-1}, and the distance of the needle from the target and the potential applied were 10 cm and 15 kV respectively.

Fibre-mats were kept in a 50% RH atmosphere for 7 days ($CDP_{f\text{-}RH}$) to allow the rehydration of the fibres to the initial CsH_2PO_4. Contact with atmospheres of higher relative humidity was avoided since these lead to progressive dissolution of the electrospun fibre surface.

A membrane electrode assembly (MEA) was prepared by sandwiching a 50 μm thick fibre mat between two Pt-loaded electrodes. These electrodes were prepared by spraying 1 mg cm^{-2} Pt black (Alfa-Aesar) onto a carbon paper gas diffusion layer (GDL) (Freudenberg H2315-C2).

2.2 Characterisation

Samples of CsH_2PO_4 (CDP), partially polymerised CDP (CDP_p), electrospun fibres (CDP_f) and rehydrated electrospun fibres ($CDP_{f\text{-}RH}$) were characterised by Powder X-Ray Diffraction (PXRD), Solid State Magic Angle Spinning Nuclear Magnetic Resonance (MAS NMR), Scanning Electron Microscopy (SEM) and Electrochemical Impedance Spectroscopy (EIS). The ohmic resistance of the fibre mat was analysed by polarisation under H_2 and N_2 in a fuel cell.

PXRD analysis of samples was conducted by a Phillips Analytical X'Pert X-ray Powder Diffractometer using Cu Kα radiation ($\lambda = 1.54180$ Å, 40 kV, 40 mA, 0.0334° 2θ step, 150 s per step). SEM analyses were carried out in a FEI XL30 ESEM-FEG microscope in low vacuum mode at 15 kV. Solid state ^1H and ^{31}P NMR analyses were performed with a Varian VNMRS 400 WideBore solid state NMR spectrometer with a Varian 3.2 mm T3 probe and 3.2 mm zirconia rotor. The electrospinning device comprised a high voltage power supply and a syringe pump to control the feed rate of CDP solution to the syringe. Proton conductivity of CDP, CDP_p and CDP_f was measured by Electrochemical Impedance Spectroscopy (EIS). EIS analyses were carried out in a 2 probe cell with platinum electrodes using a PSM1735 Multimeter analyser with a Newtons4th Ltd IAI (Impedance Analysis Interface) in the frequency range of 50 kHz–1 Hz. All the materials were ground in a mortar and pressed for 5 min at 8 tonne into a pellet of 0.5 mm thickness and 1.8 cm diameter to measure conductivity. The relative humidity in the conductivity cell was maintained between 1.5 and 4% to avoid further dehydration of the materials.[20] Each conductivity value was measured after 30 min stabilisation time. The electrochemical test was performed in a fuel cell using an EG&G Princeton scanning potentiostat model 362. The system was operated at 250 °C with humidification of 2%RH in both anode (H_2) and cathode (N_2). The polarisation curve was run at 2 mV s^{-1} in order to determine the IR contribution of the fibre mat to the electrochemical system.

3 Results and discussion

The fibre form of CDP has not been previously described and it is important to characterise its properties and behaviour and compare them with those of the bulk material to understand the viability of this method to fabricate a proton conducting medium temperature electrolyte. The chemical structure, morphology and proton conducting properties of the novel fibrous CDP were studied in order to verify that this material fulfils all the requirements needed.

Fig. 2 shows the PXRD patterns in the 2θ range of 14–32° of (a) CDP (b) CDP_f and (c) $CDP_{f\text{-}RH}$. The first of these shows the typical diffraction peaks corresponding to the room temperature monoclinic structure of CDP, with a $B21/m$ space group and lattice parameters $a = 4.8725$ Å, $b = 6.3689$ Å and $c = 15.0499$ Å.[21] In pattern (b), corresponding to CDP_f, the main peaks of the

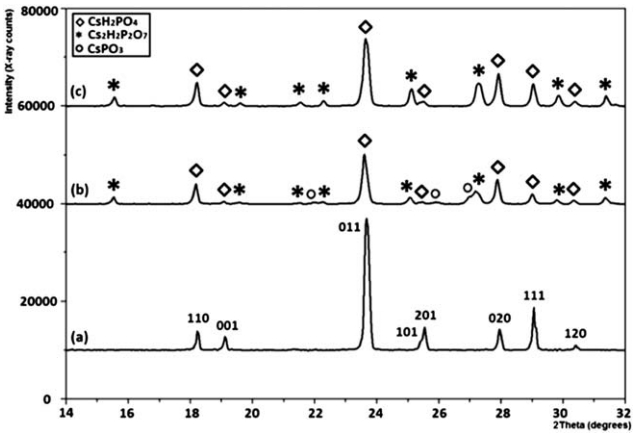

Fig. 2 X-ray diffraction patterns of (a) bulk CDP, (b) CDP_f and (c) $CDP_{f\text{-}RH}$.

initial CDP, marked with '◇', are still visible although they generally show lower intensity. New diffraction peaks attributed to formation of a new phase of partially polymerised CDP, cesium pyrophosphate ($Cs_2H_2P_2O_7$),[22–24] are shown and marked with '*'. The positions are in good agreement with the diffraction peaks reported in the JCPDS database for this material (card number: 45-619). This phase presents an orthorhombic structure with lattice parameters $a = 4.571$ Å, $b = 8.150$ Å and $c = 11.405$ Å.[25] The presence of three low intensity peaks marked with '○' suggests further polymerisation to cesium metaphosphate ($CsPO_3$),[23] with a monoclinic structure and lattice parameters $a = 12.744$ Å, $b = 4.344$ Å and $c = 6.829$ Å.[25] These peaks do not closely correspond to patterns reported in the JCPDS database for $CsPO_3$ (card number: 45-617) probably because they correspond to a different degree of condensation of phosphates.[19] It is worth noting that the left hand limb at 25.9° was described as an unknown phase diffraction peak by Taninouchi *et al.*[23] In diffraction pattern (c), corresponding to rehydrated electrospun fibres ($CDP_{f\text{-}RH}$), all the diffraction peaks corresponding to CDP and $Cs_2H_2P_2O_7$ are observed, meaning that cesium pyrophosphate does not hydrolyse to the initial CDP in the conditions applied. Nevertheless, the peaks corresponding to further polymerised species disappeared, which means that those species hydrolysed in these conditions.

According to these diffraction patterns, in CDP_f a mixture of partially dehydrated/polymerised ($Cs_2H_2P_2O_7$) and bulk (CsH_2PO_4) material coexist, although few low intensity peaks corresponding to further dehydrated species were also observed.

Considering CsH_2PO_4 and $Cs_2H_2P_2O_7$ as the major coexisting phases in the CDP fibres, a semi-quantitative Relative Intensity Ratio (RIR) method was used to estimate the mass ratio of each of the phases in the samples.[26] The values obtained for a mass ratio of phases CsH_2PO_4 : $Cs_2H_2P_2O_7$ were 69 : 31% for CDP_f and 71 : 29% for $CDP_{f\text{-}RH}$. This suggests that, although a few condensed phosphate species appear to hydrolyse, most of them remain stable at the conditions applied, which are thermodynamically more favourable for rehydration than the temperature and relative humidity conditions of an intermediate temperature electrochemical device.

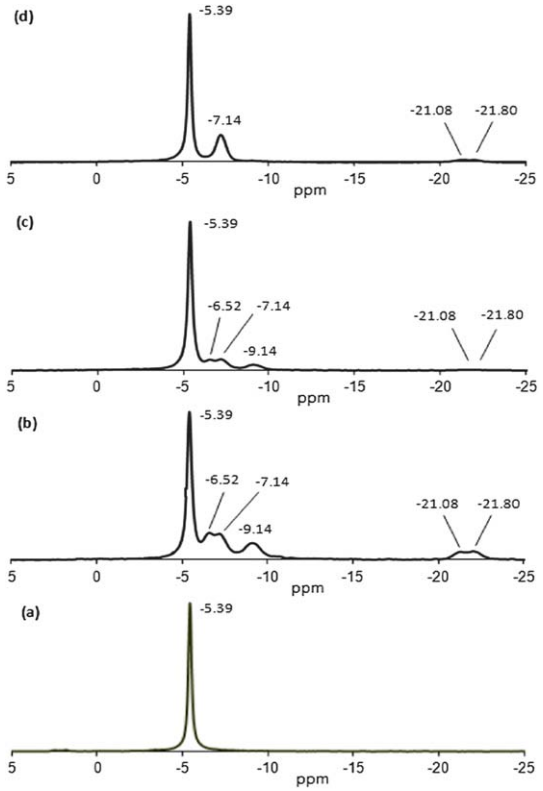

Fig. 3 ^{31}P MAS NMR spectra of (a) bulk CDP, (b) CDP_p, (c) CDP_f, and (d) $CDP_{f\text{-}RH}$.

Fig. 3 shows the ^{31}P MAS NMR spectra of (a) bulk CDP, (b) CDP_p, (c) CDP_f and (d) $CDP_{f\text{-}RH}$. The first spectrum presents a single sharp resonance with a chemical shift at −5.39 ppm which corresponds to the phosphorus of the dihydrogen phosphate group. This resonance appears also in the spectra of Fig. 3(b)–(d), indicating that dihydrogen phosphate groups are conserved in the material after partial polymerisation and electrospinning to CDP fibres. In the spectrum of CDP_p six resonances with different chemical shifts are observed at −5.39, −6.52, −7.14, −9.14, −21.08 and −22.80 ppm corresponding to different degrees of condensation of the phosphate groups. All these signals are also visible, although with lower intensity, in the spectrum of CDP_f. The lower intensity is explained by the partial rehydration of the material when dissolving it in water to prepare the electrospinning solution. In the spectrum of CDP_f after conditioning at 50% RH for 7 days, the resonances with chemical shifts at −6.65 and −9.20 disappear due to the partial hydrolysis of the condensed phosphate species.

^1H NMR spectra of bulk CDP is shown Fig. 4a. Two resonances with chemical shifts at 14.47 and 10.96 ppm are observed. These peaks correspond to the two crystallographically distinct hydrogen atoms of the dihydrogen phosphate group.[27–29] In the case of the ^1H NMR spectra of CDP_f (Fig. 4b), the same two resonances are observed with a small negative shift of approximately 0.50 ppm placing them at 13.92 and 10.55 ppm. The presence of the two same resonances in the electrospun fibres confirms that the initial bulk CDP type environment of hydrogen remains in the structure of the electrospun fibres.

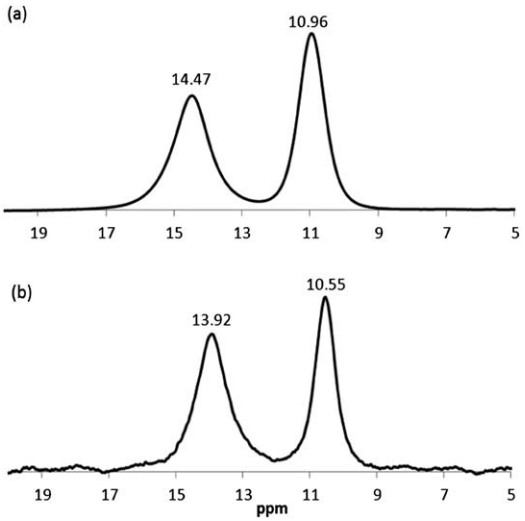

Fig. 4 ^{1}H MAS NMR spectra of (a) bulk CDP and (b) CDP_f.

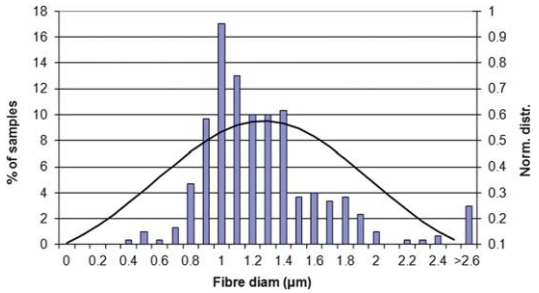

Fig. 6 Diameter size distribution of CDP_f.

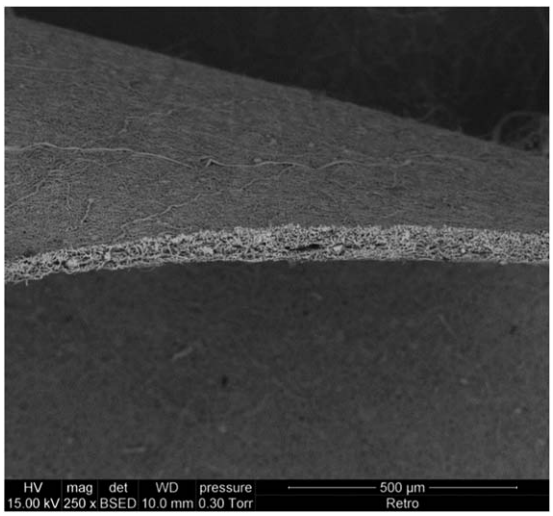

Fig. 7 SEM micrograph (250×) in cross-section of a densified CDP_f mat at 2 tonne.

Fig. 5 shows SEM micrographs of CDP, CDP_p and CDP_f. The as-prepared CDP (Fig. 5a) has smooth surfaced particles with an average diameter of 8 μm. After the polymerisation step (Fig. 5b) particles are seen to have fused together forming agglomerates of diameter >50 μm which appear to form an extended structure in three dimensions. In Fig. 5c electrospun CDP_f fibres are shown. The distribution of the fibre diameter of CDP_f, calculated by the analysis of three different regions of the mat surface with a sample size of 300 points, follows a normal distribution having its maximum at 1.25 μm, as shown in Fig. 6. The majority of the fibres are of sizes in the range of 0.5–2 μm, although some thicker fibres are also visible. These thick fibres are formed by the instabilities occurring in the Taylor cone during the electrospinning process.[30]

CsH_2PO_4 fibres fabricated by electrospinning onto the static target produce a 'cotton-wool-like' mat. This mat was pressed to densify it, and thus to reduce its porosity, using pressures from 0.5 to 4 tonne at room temperature and for 1 min for each sample. In Fig. 7 and 8 SEM micrographs of the fibre mat after densification at 2 and 4 tonne are shown. A pressure of 2 tonne (Fig. 8a) was chosen as the optimum value as it provided the highest porosity reduction while maintaining integrity of the fibres. At pressures higher than 4 tonne, fibres fused together, becoming a brittle pellet (Fig. 8b). The thickness of the fibre mat is easily controlled by the time of electrospinning and densification pressure.

The proton conductivity of the prepared materials was measured in a closed conductivity cell. Pellets of CDP, CDP_p and CDP_f with densities of 97, 95 and 98% respectively were prepared using the previously mentioned conditions.

Proton conductivities in the temperature range of 200–250 °C are plotted in Fig. 9. Here, CDP shows its characteristic behaviour with an increase in conductivity by three orders of magnitude at temperatures higher than 230 °C. In CDP_p and CDP_f the superprotonic phase transition is smoothened, and the CDP_f pellet

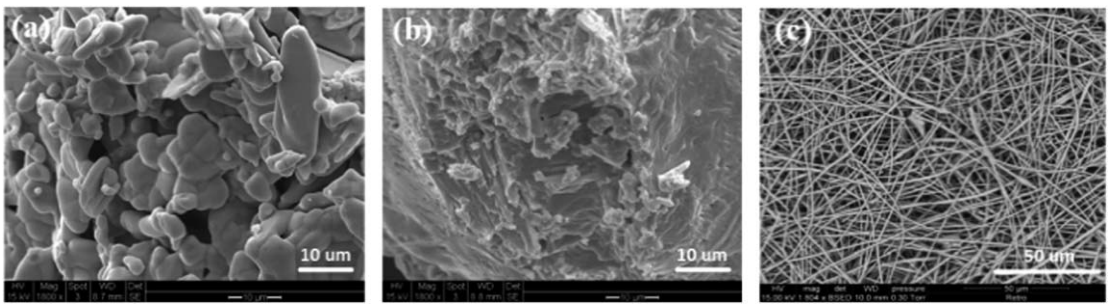

Fig. 5 SEM micrographs of (a) CDP, (b) CDP_p and (c) CDP_f.

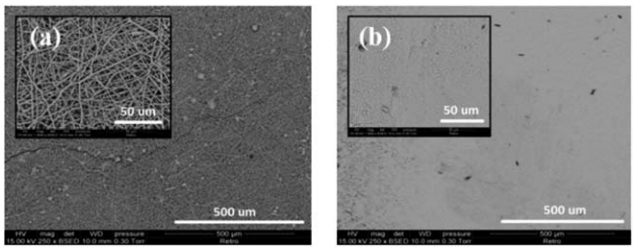

Fig. 8 SEM micrographs (250× and 1800×) of densified CDP_f mats at (a) 2 tonne and (b) 4 tonne.

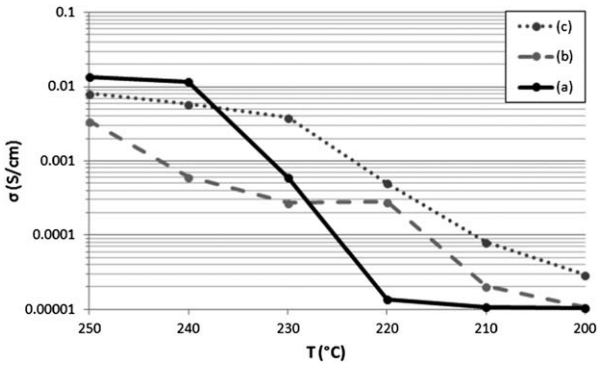

Fig. 9 Protonic conductivity as a function of temperature of (a) CDP, (b) CDP_p and (c) CDP_f.

showed a continuous increase in its proton conductivity by two orders of magnitude, from 200 to 230 °C and a more moderate increase from 3×10^{-3} S cm^{-1} to a maximum value of 8×10^{-3} S cm^{-1} at 250 °C. The partially polymerised CDP_p showed a continuous increase in conductivity of more than two orders of magnitude to a maximum value of 3.4×10^{-3} S cm^{-1} at 250 °C. The humidification in the conductivity cell was maintained between relative humidities of 1.5–4% to avoid further dehydration of the materials.[9,31] The similar behaviour of CDP_p and CDP_f with CDP corroborates the presence of the bulk CsH_2PO_4 phase in the heat-treated and electrospun samples (Fig. 10).

The resistance of the electrospun CDP fibre mat was calculated by polarisation in a fuel cell using H_2 and N_2 gases at 250 °C. The MEA was comprised of a 50 μm thickness mat sandwiched between two electrodes with 1 mg cm^{-2} Pt loading.

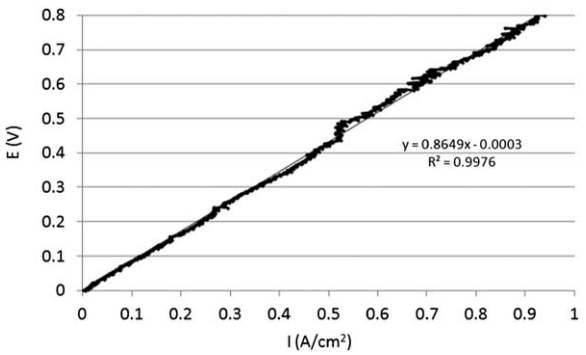

Fig. 10 H_2/N_2 polarisation of the CDP_f mat in the fuel cell at 250 °C.

The straight line observed in the fuel cell performance suggests that no substantial kinetic losses are derived from the half reactions of the system and therefore, the linear losses observed in the polarisation are mainly caused by the ohmic resistance of the mat. By calculating the slope of the line we can estimate by $R = E/I$ the resistance of the fibre mat electrolyte. By this method a resistance of 865 mΩ is calculated, which, considering the thickness of the mat, would lead to a conductivity value of 5.8×10^{-3} S cm^{-1}, in good agreement with previous conductivity measurements. The lower density of the mat compared to a dense pellet and the small kinetic loss contribution are considered to cause a lower value in the calculated conductivity.

4 Conclusions

A new fabrication method of an intermediate temperature proton conducting membrane was established. Pure inorganic CsH_2PO_4 fibres (CDP_f) were synthesised by electrospinning a viscous solution of partially polymerised CDP (CDP_p). This method provides a way to fabricate pure inorganic fibres in the absence of a carrier polymer. X-ray diffraction and MAS NMR analysis suggest that different phases of CDP, corresponding to different degrees of polymerisation, coexist in the fibres. The electrospun CDP_f showed a maximum proton conductivity of 8×10^{-3} S cm^{-1} at 250 °C which makes them of potential use in an intermediate temperature electrochemical device. A dense proton conducting fibre mat of required thickness can be then produced which can be subsequently reinforced by the addition of a polymer to produce a robust composite membrane.

Acknowledgements

This research was supported by the European Commission through the ITN project SUSHGEN number 238678. Solid-state ^{1}H NMR spectrum of CsH_2PO_4 (Fig. 4a) was obtained at the EPSRC UK National Solid-State Service at Durham.

Notes and references

1 A. Goñi-Urtiaga, D. Presvytes and K. Scott, *Int. J. Hydrogen Energy*, 2012, **37**, 3358–3372.
2 S. Hart, P. W. Richter, J. B. Clark and E. Rapoport, *J. Solid State Chem.*, 1981, **37**, 302–307.
3 A. I. Baranov, L. A. Shuvalov and N. M. Shchagina, *Journal of Experimental and Theoretical Physics Letters*, 1982, **36**, 459.
4 A. I. Baranov, V. P. Khiznichenko and L. A. Shuvalov, *Ferroelectrics*, 1989, **100**, 135–141.
5 P. Colomban, *Proton conductors: Solids, membranes and gels – materials and devices*, 1992.
6 S. M. Haile, D. A. Boysen, C. R. I. Chisholm and R. B. Merle, *Nature*, 2001, **410**, 910–913.
7 D. A. Boysen, S. M. Haile, H. Liu and R. A. Secco, *Chem. Mater.*, 2004, **16**, 693–697.
8 B. Anshumaan, C. Vaibhaw Singh and S. P. Raj Ganesh, *Advances in solid acid electrolytes for fuel cell applications*, 2012.
9 D. A. Boysen, T. Uda, C. R. I. Chisholm and S. M. Haile, *Science*, 2004, **303**, 68–70.

10 S. M. Haile, C. R. I. Chisholm, K. Sasaki, D. A. Boysen and T. Uda, *Faraday Discuss.*, 2007, **134**, 17–39.
11 C. R. I. Chisholm, D. A. Boysen, A. B. Papandrew, S. Zecevic, S. Cha, K. A. Sasaki, Á. Varga, K. P. Giapis and S. M. Haile, *Electrochem. Soc. Interface*, 2009, 53–59.
12 J. Otomo, T. Ishigooka, T. Kitano, H. Takahashi and H. Nagamoto, *Electrochim. Acta*, 2008, **53**, 8186–8195.
13 H. Muroyama, K. Kudo, T. Matsui, R. Kikuchi and K. Eguchi, *Solid State Ionics*, 2007, **178**, 1512–1516.
14 V. G. Ponomareva and E. S. Shutova, *Solid State Ionics*, 2007, **178**, 729–734.
15 V. G. Ponomareva, N. F. Uvarov, G. V. Lavrova and E. F. Hairetdinov, *Solid State Ionics*, 1996, **90**, 161–166.
16 H. Muroyama, K. Kudo, T. Matsui, R. Kikuchi and K. Eguchi, *Solid State Ionics*, 2007, **178**, 1512–1516.
17 S. Cavaliere, S. Subianto, I. Savych, D. J. Jones and J. Roziere, *Energy Environ. Sci.*, 2011, **4**, 4761–4785.
18 Z.-M. Huang, Y. Z. Zhang, M. Kotaki and S. Ramakrishna, *Compos. Sci. Technol.*, 2003, **63**, 2223–2253.
19 K.-S. Lee, *J. Phys. Chem. Solids*, 1996, **57**, 333–342.
20 D. A. Boysen, T. Uda, C. R. I. Chisholm and S. M. Haile, *ChemInform*, 2004, **35**(14).
21 R. J. Nelmes and R. N. P. Choudhary, *Solid State Commun.*, 1978, **26**, 823.
22 E. Ortiz, R. A. Vargas and B. E. Mellander, *Solid State Ionics*, 1999, **125**, 177–185.
23 Y.-k. Taninouchi, T. Uda, Y. Awakura, A. Ikeda and S. M. Haile, *J. Mater. Chem.*, 2007, **17**, 3182–3189.
24 Y. Taninouchi, N. Hatada, T. Uda and Y. Awakura, *J. Electrochem. Soc.*, 2009, **156**, B572–B579.
25 V. Bronowska, *International Centre for Diffraction Data*, JCPDS, 1997.
26 F. H. Chung, *J. Appl. Crystallogr.*, 1974, **7**, 526–531.
27 J. W. Traer, K. J. Soo, M. Vijayakumar and G. R. Goward, *J. Phys. Chem. C*, 2011, **115**, 6064–6072.
28 S. M. Haile, H. Liu and R. A. Secco, *Chem. Mater.*, 2003, **15**, 727–736.
29 K. Yamada, Y. Sagara, Y. Yamane, H. Ohki and T. Okuda, *Solid State Ionics*, 2004, **175**, 557–562.
30 D. H. Reneker, A. L. Yarin, E. Zussman and H. Xu, *Adv. Appl. Mech.*, 2007, **41**, 43.
31 J. Otomo, T. Tamaki, S. Nishida, S. Wang, M. Ogura, T. Kobayashi, C.-j. Wen, H. Nagamoto and H. Takahashi, *J. Appl. Electrochem.*, 2005, **35**, 865–870.